

Review of Petrophysical characterization of the lacustrine sediment succession drilled in Lake El'gygytyn, Far East Russian Arctic

by A. C. Gebhardt¹, A. Francke², J. Kück³, M. Sauerbrey², F. Niessen¹, V. Wennrich², and M. Melles²

The manuscript is one a series resulting from a comprehensive lake drilling program, undertaken in a unique setting and under extreme environmental and operational conditions. No doubt it will be an enduring key paleoclimate reference site. This paper synthesizes an extensive suite of physical properties, seismic, downhole geophysical, and bulk geochemical data. Some of the key datasets integrated were previously published (seismic, geochemical data) but this seems to be the first paper dedicated to assessing the physical properties of drilled and recovered core material.

Importantly, the downhole data analysis reflects the lower 2/3 of the section drilled, as measurements of upper section were either compromised or not acquired, evidently due to abandoned pipe left in nearby drillholes.

The principal quantitative synthesis approach is a type of cluster analysis (k-means), which is one reasonable approach to quantifying downhole lithology and deriving inferences accordingly (PCAS is more commonly applied but this works fine). The specific purpose of the statistical analysis should be explicitly stated early on in the paper however.

It is not clear if the seismic reflection data presented were single-fold Bolt airgun records, or multifold GI gun data....this should be clarified.

It would be useful to the reader if the authors could post detailed ages directly onto the seismic reflection profiles at the drill site. A zoomed-in image of reflection seismic data at the drill hole with this age info would be helpful.

The standard approach for directly correlating reflection seismic data to drill holes is to generate synthetic seismograms using density and velocity data. Although their downhole tool failed during operations, velocity data from the whole-core logs should be available, and following data conditioning could be used to tying the drill hole to the seismic data. I recommend this be considered in the context of this paper.

The U-peaks are intriguing. Is it possible there is a relationship between U and high-TOC intervals? This cannot be determined from figures as presented....please consider including downcore TOC along with U on Figure. 3.

4.2 and 4.3 have identical subtitles (also 5.1 and 5.2).....please change/clarify each section.

The conceptual model of colder periods of high ice cover producing enhanced siliciclastic inputs seems a bit problematic; perhaps given the high resolution of most of these data sets this could be refined?

Scientific Significance - Good

Scientific Quality - Excellent

Presentation Quality - Good

Responses to Editorial Queries

1. **Does the paper address relevant scientific questions within the scope of CP?** Yes
2. **Does the paper present novel concepts, ideas, tools, or data?** Yes this contains new data synthesized with key previously published data.
3. **Are substantial conclusions reached?** Yes. The broad results are largely non-unique compared to recently published paper in Science, but provide an essential perspective and new details on this long record high-latitude terrestrial record.
4. **Are the scientific methods and assumptions valid and clearly outlined?** Yes. Data analyses are rigorous and justified.
5. **Are the results sufficient to support the interpretations and conclusions?** Yes.
6. **Is the description of experiments and calculations sufficiently complete and precise to allow their reproduction by fellow scientists (traceability of results)?** Yes, note remarks above.
7. **Do the authors give proper credit to related work and clearly indicate their own new/original contribution?** Yes.
8. **Does the title clearly reflect the contents of the paper?** Yes.
9. **Does the abstract provide a concise and complete summary?** Yes.
10. **Is the overall presentation well-structured and clear?** Mostly. Several subsection titles are repeated, and need to be clarified (see above).
11. **Is the language fluent and precise?** The paper is mainly well-written but requires further editing. In a few places it the text is verbose (see marked-up copy). The authors should take care to avoid the vernacular and informal prose (many instances of this in the text....see mark-up). For example:

“probe *basically* consists of

“While electrical resistivity shows pronounced peaks in the bedrock and in the transitional zone, it is *pretty* constant with only very small peaks throughout the entire lacustrine section,...”;

Authors need to take care in usage of “further” (as in meaning, for instance, additional study) versus “farther” ((as in implying additional physical distance).

Suggest that the authors avoid parenthetical statements.

Suggest that the authors avoid writing in the first person, as is done in many places in text.

12. **Are mathematical formulae, symbols, abbreviations, and units correctly defined and used?** Yes.
13. **Should any parts of the paper (text, formulae, figures, tables) be clarified, reduced, combined, or eliminated?** Yes, see above.
14. **Are the number and quality of references appropriate?** Yes.
15. **Is the amount and quality of supplementary material appropriate?** N/A.

Abstract

Seismic profiles of Far East Russian Lake El'gygytyn, which was formed by a meteorite impact some 3.6 million years ago, show a stratified sediment succession that can be separated into Subunits Ia and Ib at approximately 167 m below lake floor (= ~3.17 Ma). The former is well-stratified, while the latter is acoustically more massive. The sediments are intercalated with frequent mass movement deposits mainly in the proximal ^{central} part, while the distal ^{part} is almost free of such deposits at least in the upper part. In spring 2009, a long core drilled in the lake center within the framework of the International Continental Scientific Drilling Program (ICDP) penetrated the entire lacustrine sediment succession down to ~320 m below lake floor and about 200 m ^{farther} into the meteorite-impact related bedrock. Downhole logging data down to 390 m below lake floor show that the bedrock and the lacustrine part of the core differ ^{significantly} largely in their petrophysical characteristics. The contact between the bedrock and the lacustrine sediments is not abrupt, but rather transitional with a ^{variable} mixture of impact-altered bedrock clasts in a lacustrine matrix with ^{varying} percentages. Physical and chemical proxies measured on the cores can be used to divide the lacustrine part into five different clusters. These can be plotted in a redox-condition vs. input type diagram with total organic carbon content and magnetic susceptibility values indicating anoxic or oxic conditions and with the Si/Ti ratio representing more clastic or more biogenic input. Plotting the clusters in this diagram allows identifying clusters that represent glacial phases (Cluster I), super interglacials (Cluster II), and interglacial phases (Clusters III and IV).

1 Introduction

The Arctic region is ^{highly} strongly susceptible to global change and, at the same time, plays a major role in the global climate system through feedback processes in the oceans, the atmosphere, and the cryosphere. It is ~~thus~~ ^{thus, of importance} to understand past climate changes under different climate-forcing conditions, in order to make

Accordingly it is important

The Page

Abstract

Introduction

Conclusions

References

Tables

Figures

1

2

3

4

Back

Close

Full Screen / Esc

Printer-friendly Version

Interactive Discussion



about

accurate predictions of future climate development. Lakes of the higher latitudes are still sparsely investigated even though they are highly sensitive to shifts in climatological and environmental conditions (e.g. temperature, precipitation, insolation, vegetation, ice coverage), and as such they are valuable tracers of climate change. This lack of investigation is mainly due to their remote location and logistical problems of reaching these study sites. Lakes in the high Arctic are often characterized by long winters resulting in long periods of ice coverage, followed by a short open water season. Furthermore, many lakes of the high Arctic are subject to glacial overprint and potentially do not contain longterm terrestrial paleoclimate records.

Lake El'gygytyn (Fig. 1) provides a unique opportunity to investigate paleoclimate conditions of the Arctic realm reaching back 3.6 million years (approximately one million years prior to the first major glaciation of the Northern Hemisphere), but it provides a resolution to resolve climate fluctuations on orbital to centennial time scales (Melles et al., 2012). Until now, only a few terrestrial records with such a high temporal resolution are known from the Arctic realm (e.g. the Greenland ice cores, Dansgaard et al., 1993; Grootes et al., 1993; Svensson et al., 2011; NGRIP members, 2004), but none of them reaches back to the onset of the Northern Hemisphere glaciation continuously. Marine records of the Arctic Ocean in general reach back much further in time, but show a lower temporal resolution (e.g. Lomonosov Ridge, Moran et al., 2006; Yermak Plateau, Myhre et al., 1995).

Lake El'gygytyn is one of only a handful of lakes that formed inside a meteorite impact crater (Lerman et al., 1995). When the meteorite hit the target area 3.6 million years ago (Layer, 2000), the Northern Hemisphere experienced the rather constant, moderate to warm climate of the mid-Pleistocene (Harris, 2005; Repenning and Brouwers, 1987). According to Harris (2005), the Arctic Ocean was unfrozen at that time, and Boreal cedar forests covered the landside along the Arctic Ocean coasts (Repenning and Brouwers, 1987). At around 3 million years before present, the Boreal forests were replaced by tundra around the Bering Strait and inland (Harris, 2005, and references therein). Herman and Hopkins (1980) reported a sharp change in the

9. 351–391, 2013

Petrophysical characterization of the lacustrine sediment succession

A. C. Gebhardt et al.

*number of avoid potential
claims if possible*

This Page

Abstract

Introduction

Conclusions

References

Tables

Figures

1

2

3

4

Back

Close

Full Screen Esc

Printer-friendly Version

Interactive Discussion



sedimentation regime as well as the first occurrence of ice rafted debris (IRD) in the Arctic Ocean from about 2.53 Ma, and the onset of large-scale glaciation in Scandinavia (by means of a marked increase in IRD flux) was dated to 2.75 Ma by Fronval and Jansen (1996) and Jansen et al. (2000). Since then, the Arctic realm has experienced several advances and retreats of glaciers and ice sheets. A dropstone which was found in sediments as old as 45 Ma and the frequent occurrence of IRD since the early Miocene in a marine record from the Lomonosov Ridge, however show that the onset of the transition from a greenhouse world to colder climate with sea ice and icebergs might have begun much earlier than hitherto assumed (Moran et al., 2006).

The El'gygytgyn area was never subject to glacial overprint since its formation (Glushkova and Smirnov, 2007) and, thus, the lake contains an undisturbed climate record of approximately 3.6 million years, unique for the terrestrial Arctic realm. This record was drilled within the framework of the International Continental Scientific Drilling Program (ICDP). A permafrost core (ICDP Site 5011-3) was retrieved from the eastern shoreline in late autumn 2008, and during winter/spring 2009, a 517 m long drill core (ICDP Site 5011-1) containing lacustrine sediments and the impact-related bedrock underneath was retrieved from the ice cover of the lake (Melles et al., 2011).

This paper aims at characterizing the lacustrine part of core 5011-1 as well as the transitional zone between the lacustrine sediments and the impact-related bedrock by means of petrophysical parameters such as physical properties and downhole logging measurements. These findings are then compared to the facies description by Melles et al. (2007, 2012) and their interpretation *contained therein*.

2 General settings of the investigation area

2.1 Study area

Lake El'gygytgyn (67° 30' N, 172° 05' E) is located about 100 km north of the Arctic Circle in Central Chukotka, NE Russia (Fig. 1). It was formed by a meteorite impact

that was dated using $^{40}\text{Ar}/^{39}\text{Ar}$ to about 3.6 million years (Layer, 2000; Gurov et al., 1979a, b; Belyi, 1998). The lake's surface lies at about 490 m a.s.l. and the surrounding crater rim reaches ^{elevation} altitudes of 900 to almost 1000 m a.s.l. $\sim 900-1000 \text{ m a.s.l.}$

The lake is roughly circular with a diameter of 12 km. Its catchment is limited to the crater rim (293 km² in total, including lake surface) with about 50 small ephemeral creeks draining into the lake (Nolan and Bringham-Grette, 2007). The Enmyvaan River at the southern edge of the lake is its only outflow (Fig. 1a). The lake has a bowl-shaped form with a flat, central plain of 170 m water depth and flanks that are steepest in the northern and northeastern part. A shelf of 10 to 12 m water depth has developed in the southeastern, southern, and southwestern to western ^{edges} part of the lake (Fig. 1a).

The lake is presently ice-covered during 9–10 months ^{on average} with only a short period of completely open water (Nolan and Bringham-Grette, 2007). During the short summer season, the monomictic and ultra-oligotrophic lake gets mixed completely (Nowaczyk et al., 2002; Nolan and Bringham-Grette, 2007). The catchment vegetation consists mainly of moss-tundra interspersed by few shrub willows; the modern tree line lies about 150 km further south and west (Nowaczyk et al., 2002). The current wind system ~~has~~ is a bipolar mode with winds approximately from north and south, respectively (Nolan and Bringham-Grette, 2007).

2.2 Lithological succession

The impact crater shows internal geometries as expected for a crater of its size; a central uplift structure interpreted in the form of a central uplift ring structure was revealed by seismic refraction data; it is overlain by an impact breccia (suevite) (Gebhardt et al., 2006). The lacustrine sediments can be divided into two units by means of refraction data; the upper unit is characterized by a seismic velocity of 1550 m s^{-1} and a thickness of about 170 m, the lower unit by 1650 m s^{-1} and a variable thickness of 190 m on top of the uplift ring structure to 290 m in the surrounding basin (Gebhardt et al., 2006). Mass movements (slides, debris flows, and turbidites) are a common feature mainly in proximal ^{regions} parts of the lacustrine sediments. These mass movement

9, 351–391, 2013

Petrophysical characterization of the lacustrine sediment succession

A. C. Gebhardt et al.

Title Page

Abstract

Introduction

Conclusions

References

Tables

Figures

1

2

3

4

Back

Close

Full Screen / Esc

Printer-friendly Version

Interactive Discussion

CC BY

packages have already been described as massive, acoustically transparent sediment bodies by Niessen et al. (2007) from high-resolution 3.5 kHz seismic data. Gebhardt et al. (2005) distinguished between two types of mass movement sediments: deposits with a distinct "nose" at their front end, forming a well-defined distal border, and deposits that gradually pinch out, forming a diffuse distal border, poorly visible in the profiles. Melles et al. (2007) report fine-grained turbidites from the pilot core recovered in 1998 (PG1351; Fig. 1). A detailed study of four cores along a transect from the lake border towards the center by Juschus et al. (2009) demonstrated that initial slope failures transform into erosive debris and/or grain flows during their advance, and accumulate as non-erosive turbidites in the lake center. This process of suspension settling out is also known from other lakes (e.g. Eyles et al., 2003; Finckh et al., 1984; Van Rensbergen et al., 1998, 1999). Whilst only turbidites and grain flow deposits reached the lake center during the studied ~ 350 ka of pilot cores PG1351 and LZ1024 (Juschus et al., 2009; Frank et al., 2013), investigations of the long 5011-1 cores have revealed several slides, slumps and debrites in deeper core sections (Sauerbrey et al., 2013). Slides, slumps, grain and debris flows can be recognized in the seismic sections, but turbidite sequences are rather thin and, thus, beyond resolution of the seismic data. Mass movement deposits make up approximately one third of the entire lacustrine record drilled in the lake. They were extensively studied by Sauerbrey et al. (2013).

In spring 2009, three drill cores were retrieved from the center of Lake El'gygytyn (Site 5011-1, cores 5011-1A, 1B, 1C) down to a maximum depth of 517.3 m below lake floor (b.l.f.). A detailed description of all drilling details is given by Melles et al. (2011). The cores were transported to the laboratory facilities at the University of Cologne, Germany, where they were opened and described. Based on the core description together with several proxies, a composite profile was composed (Melles et al., 2012; Nowaczyk et al., 2013). The composite sediment core mainly consists of highly variable silty-clayey pelagic sediments divided into different facies types by Melles et al. (2012) and Bringham-Grette et al. (2013), interfingered with mass movement deposits (Sauerbrey et al., 2013).

9, 351–391, 2013

Petrophysical characterization of the lacustrine sediment succession

A. C. Gebhardt et al.

Title Page

Abstract

Introduction

Conclusions

References

Tables

Figures

1

2

3

4

Back

Close

Full Screen / Esc

Printer-friendly Version

Interactive Discussion



“Facies A” consists of fine clastic laminations of less than 5 mm thickness (average is ~0.2 mm). The sediments of facies type A are mainly dark gray to black in color. This points at a stratified water column and anoxic bottom water conditions (Melles et al., 2012). The authors associate this facies type with peak glacial conditions and a perennial ice cover of the lake with mean annual air temperatures of at least 4 (± 0.5) °C less than today. This facies was already described in pilot core PG1351 as subunits 3 (“cold & dry”) and 4 (“cold & moist”), characterized by enhanced amounts of total organic carbon (TOC), medium to low biogenic silica content (Melles et al., 2007), and low magnetic susceptibility due to dissolution of magnetite by anoxic conditions (Nowaczyk et al., 2007). The “cold & dry” subtype is further referred to as A_d , “cold & moist” as A_m . Facies A sediments are limited to the younger part of the sediment record (Brigham-Grette et al., 2013), i.e. the uppermost ~124 m (\approx 2.6 Ma).

“Facies B” is the most abundant facies type in the composite profile and mainly consists of olive gray to brown, massive to faintly banded silt with greenish bands of typically 1–3 cm thickness. The sediments are characterized by a lack of sedimentary structures, pointing at bioturbation and oxygenated bottom water (Melles et al., 2012). This implies warmer climate with ice-free summers and a mixed water column. This facies reflects a wide range of glacial to interglacial settings including the modern situation. TOC content is rather low in facies type B due to high organic matter decomposition in oxic bottom water conditions; biogenic silica values are intermediate to high due to enhanced primary productivity, and magnetic susceptibility is high reflecting good preservation of magnetite (Melles et al., 2012).

“Facies C” is the least common facies type found in the composite profile (Melles et al., 2012). It is irregularly distributed and consists of distinctly reddish-brown silt. Melles et al. (2012) suggest oxidation of bottom sediments by a well-ventilated water column as responsible for the distinct reddish color. This facies type was interpreted as “super interglacial” conditions, e.g. during extraordinary warm MIS11 and 31 (Melles et al., 2012). Distinct laminae are found in facies type C, probably pointing at winter stratification and anoxic bottom water conditions under a seasonal ice cover. This is

Petrophysical characterization of the lacustrine sediment succession

A. C. Gebhardt et al.

Title Page	Abstract	Conclusions	Tables	Introduction	References	Figures
	◀	▶	◀	▶	▶	▶
Back				Close		
Full Screen / Esc						
Printer-friendly Version						
Interactive Discussion						



further supported by high TOC values. Biogenic silica content is also exceptionally high due to diatom blooms probably caused by enhanced nutrient influx from the catchment. Magnetic susceptibility is rather low both due to dissolution of the magnetic susceptibility signal by the high biogenic silica content and partial dissolution of magnetite during periods (winters) with anoxic bottom water conditions.

“Facies D” is laminated similar to Facies A, but its laminae are significantly ^{thicker} larger with an average thickness of up to ~ 1 cm. Laminae are characterized by distinct lower boundaries and a coarsening upward sequence from silt to clay with a higher total clay content than in Facies A. Facies D is mostly gray but has some red and green hues in its oldest parts. The well-preserved lamination ^{3.0-4.5 m} points ^{at a lack of bioturbation of the} bottom sediment, and the characteristic coarsening upward ^{sequence} in each lamina suggests repeated pulses of sediment delivery to the lake, probably due to variations in fluvial input (Brigham-Grette et al., 2013). Facies D is limited to the Pliocene part of the record with the youngest occurrence at ~ 141 m b.l.f. (≈ 2.9 Ma).

“Facies E” comprises the transition from the impact-altered bedrock to lacustrine sediments. This transition is more/less gradual with sediments composed of impact breccia and impact melt blocks in a matrix of lacustrine sediments, with the bedrock-related particles being dominant in the lower and the lacustrine sediments in the upper part (Koeberl et al., 2012; Raschke et al., 2012).

“Facies F” comprises a wide variety of mass movement deposits, ^{such as} ~~jet~~ turbidites, debrites, slumps, slides and grain flows. A detailed description of the mass movement deposits and their distribution within the record is given by Sauerbrey et al. (2013). Only thin mass movement ^{0.4-1.0 m} deposits (< 5 cm in thickness) were sampled in the composite profile of 5011-1, ^{thicker} thicker ones were omitted. These thinner mass movement deposits are almost exclusively turbidites.

3 Data acquisition and processing

3.1 Seismic data

Prior to deep drilling, two seismic ~~pre-site~~ surveys were carried out in ~~summers~~ 2000 and 2003. In 2000, a single-channel survey was carried out using a Bolt 600B 5 airgun (82 cm³, 6 s shot interval resulting in approximately 8 m shot distance) with a 20-element single-channel hydrophone streamer (Geacoustics AE5000) as receiver (Niessen et al., 2007). Single-channel reflection data were bandpass-filtered (100-150-350-450 Hz), and an AGC was used for display. In 2003, ~~2~~ ^{two} single-channel and an ~~ad-~~ditional ~~8~~ ^{eight} multi-channel profiles were acquired using a Mini-GI gun triggered in G-gun 10 mode at a pressure of 110 bar (426 cm³ ^{volume}, 10 s shot interval resulting in approximately 12 m shot distance). For the multi-channel profiles, a 14-channel streamer with an off-set of 130 m and a hydrophone spacing of 10 m was used as receiving array (details are given in Niessen et al., 2007). Multi-channel data were processed in a standard sequence including bandpass filtering (70-90-240-300 Hz), velocity analysis, CMP stacking, and predictive deconvolution. Tracklines are shown in Fig. 1.

3.2 Physical properties development

Physical properties data of cores 5011-1A, 1B and 1C were acquired using a Geotek Multi-Sensor Core Logger (MSCL; Geotek Ltd., UK) both in the field laboratory during the drilling campaign in 2009 (magnetic susceptibility measurements on whole cores) and at the Alfred Wegener Institute (AWI) in Bremerhaven, Germany between October 2009 and January 2011 (density measurements on split cores). The data were complemented with density and magnetic susceptibility data from pilot core Lz1024 which were measured at AWI in March/2004 on whole cores.

~~Magnetic~~ susceptibility (MS) was measured in SI units using a Bartington MS-2 meter equipped with a loop sensor of 80 mm internal diameter. Data correction was done with respect to the specific core and loop sensor diameters according to the Bartington

Manual (Geotek, 2000). Even though temperature inside the field lab container was sometimes variable due to opening and closing of the door with inside temperatures around +20 °C and outside temperatures ^{was} between -45 and -20 °C, no severe drifting of the temperature-sensitive sensor ~~could be~~ observed. The small drifting that occurred was significantly lower than the lowest susceptibility readings and, thus, did not affect the data. Both magnetic susceptibility and density data were corrected for outliers and composite profiles were spliced accordingly to the sampling scheme used for the discrete samples (Wennrich et al., 2013)

"Gamma-ray density (GRA)" was measured using a ¹³⁷Cs source mounted on the Geotek MSCL. For density calibration, standard core-size semi-cylinders consisting of different proportions of aluminum and water were logged prior to the cores according to the method described by Best and Gunn (1999) but modified for split cores. Split cores were only approximately 33 mm thick, which is beyond of what ^{the} ~~our~~ Geotek MSCL can measure reliably. To convert raw gamma ray attenuation counts to density, however, exact thickness measurements are required. ^{A secondary} ~~We therefore~~ used the surface scans that were measured by the ITRAX XRF core scanner (COX Analytical Systems, Sweden) at the University of Cologne (see Wennrich et al., this volume) in the course of the XRF measurements on the same split cores. These surface scans were calibrated for thickness using a semi-cylindrical piece with a radius of 33.15 mm to simulate a standard split core, and three pieces that were thicker (+10 mm, +20 mm) or thinner (-10 mm) than the standard to calibrate the entire range of possible sediment thicknesses. GRA was calculated using ^{Standard} ~~the method~~ described in the ~~Geotek manual~~ (Geotek, 2000).

3.3 Downhole logging data

While drilling hole 5011-1-C, operations were stopped four times to allow for the acquisition of downhole logging data. All data presented here were acquired using slimhole probes manufactured by Antares (Germany). Operation of the probes under the extreme conditions of an Arctic winter drilling campaign went overall well but also took ~~its toll with one probe completely broken~~ (acoustic velocity probe) and another partially ^{in the damaging of two probes} ~~including the~~ ³⁶⁰

Petrophysical characterization of the lacustrine sediment succession

A. C. Gebhardt et al.

Title Page

Abstract

Introduction

Conclusions

References

Tables

Figures

1

2

3

4

Back

Close

Full Screen / Esc

Printer-friendly Version

Interactive Discussion



and the damaged (caliper probe). For downhole logging sessions, the pipe was pulled out of the hole (except for the uppermost approximately 20 m where the casing was pushed into the sediment for stabilization) leaving a sufficiently stable borehole wall. After downhole logging sessions were finished, the pipes were redeployed, and drilling operations were resumed. For drilling operations, bentonite was used as drilling fluid. Downhole logging was carried out to a maximum depth of 394 m below lake floor. In order to fit the downhole logging depths to the composite profile depths, the entire downhole logging dataset was shifted downwards by 3 m. This results in an apparent discrepancy with depths used by the community that is working on the impact-related bedrock (e.g. Koberl et al., 2012; Raschke et al., 2012); ~~we therefore also shifted their depths by 3 m downwards for comparison with our data.~~ ^{accordingly these were also shifted}

Electrical resistivity and magnetic susceptibility data of the uppermost approximately 143 m could not be used as they were disturbed by the pipes of nearby abandoned holes 1A and 1B.

“Electrical resistivity (ER)” of the surrounding sediments/rock at two different lateral distances from the borehole wall (deep ~ 60 cm and shallow ~ 20 cm, with the actual penetration depending on rock porosity and the resistivity of fluid and rock) was measured using a dual laterolog probe. The probe has a vertical resolution of approximately 10 cm (electrode length: 8 cm) ^{and} typical logging speed was 12 mm min⁻¹.

⁽¹⁾ Borehole magnetic susceptibility (BMS) was measured using a probe that basically consists of a receiver coil and a transmitter coil that is located 20 cm above the former inside a non-magnetic pressure housing. The transmitter coil induces a 1 kHz alternating magnetic field. Magnetic susceptibility was corrected for the two different borehole diameters drilled during the Lake El'gygytyn deep drilling project. Down to 274.33 m composite depth (i.e. 443 m below lake surface), a bit size of 124 mm was used; a correction factor of 1.4 was applied for this ^{section} part. In the deeper part of the hole, a smaller bit size of 98 mm was used for drilling/coring, and accordingly, a correction factor of 1.25 was used. The vertical resolution is approximately 20 cm (detector spacing), but relative

variations can be identified with a resolution of about 5 cm. Penetration is ~20 cm, typical logging speed was 8–10 m min⁻¹.

The total amount of naturally occurring radioactive radiation (GR) was measured using a total natural gamma ray probe. This GR probe was always run with any other probe for depth corrections. One GR curve was chosen as the reference (Master-GR), and all other GR curves with their attached other measurements were shifted to fit the Master-GR. Vertical resolution is approximately 10 cm, typical penetration into the rock is about 10 cm.

The “spectrum of the naturally occurring radioactive radiation (SGR)”, i.e. Uranium, Thorium, and Potassium, was measured using a natural gamma ray probe. Logging speed was not faster than 2 m min⁻¹ for the SGR probe to allow gathering of a reliable gamma ray spectrum. Vertical resolution is ~10 cm, and penetration into the rock is about 15 cm. Gamma rays penetrate steel casing, therefore both the GR and the SGR probes could be run in cased holes. Corrections were carried out for the casing as well as for the different diameters of the borehole. Th and K values are often used for a first estimate and characterization of clay content in the sediments (e.g. Wonik, 2001; Ruffell and Worden, 2000; Schnyder et al., 2006) assuming that they are almost exclusively present in this grain-size fraction, and that K and Th are present in montmorillonite, illite, and kaolinite in different portions. To estimate the clay content in Lake El’gygytyn sediments, we used the approaches given by Wonik (2001):

$$C_{cl}(K) = \frac{K - K_{sand}}{K_{clay} - K_{sand}}, \quad (1)$$

and

$$C_{cl}(Th) = \frac{Th - Th_{sand}}{Th_{clay} - Th_{sand}}, \quad (2)$$

with C_{cl} = clay content (%), K_{sand} and Th_{sand} = K and Th content of sand, K_{clay} and Th_{clay} = K and Th content of clay. K and Th contents of sand are normally very low

Petrophysical characterization of the lacustrine sediment succession

A. C. Gebhardt et al.

Title Page

Abstract

Introduction

Conclusions

References

Tables

Figures

◀

▶

◀

▶

Back

Close

Full Screen / Esc

Printer-friendly version

Interactive Discussion



and were set to 0.1 % for K and 0.1 ppm for Th; K and Th contents of clay were set to the maximum K and Th values measured in the record, which is 4.5141 % for K and 22.4249 ppm for Th. K and Th in Eqs. (1) and (2) are the actual readings from the SGR dataset. A third approach uses the GR data as follows (Wonik, 2001):

$$V_{cl}(GR) = 0.33 \cdot \left(2^{2 \cdot GRI} - 1 \right), \quad (3)$$

$$GRI = \frac{GR - GR_{sand}}{GR_{clay} - GR_{sand}}, \quad (4)$$

with V_{cl} = percentage of the volume of clay, $GR_{sand} = 135$ API and $GR_{clay} = 10$ API; GR in Eq. (4) is the actual reading from the GR dataset.

3.4 Si/Ti, TOC data

Silicia/titanium (Si/Ti) ratios were determined on core halves using an X-ray fluorescence (XRF) core scanner (ITRAX, Cox Ltd., Sweden). Details on the scanner settings and processing of the data are given in Wennrich et al. (2013). Total organic carbon (TOC) content was calculated as the difference between total carbon and total inorganic carbon using a DIMATOC 200 carbon analyzer (Dimatec Corp.) in aqueous suspension.

3.5 Statistical analyses

Statistical analyses were carried out using Matlab® and the implemented statistical toolbox (Mathworks Inc., Version 7.14.0.739). In a first step, downhole logging data (magnetic susceptibility, electrical resistivity, U counts, Th counts, K counts) were clustered into 3 groups (Clusters 1 to 3) using k-mean clustering to allow for a first characterization of the entire record. Data < 143 m b.l.f. were omitted due to the disturbed magnetic susceptibility and electrical resistivity signal. In a second step, Si/Ti ratios, magnetic susceptibilities and TOC percentages measured on the composite core down

Title Page

Abstract

Introduction

Conclusions

References

Tables

Figures

1

2

3

Back

4

5

Close

Full Screen Esc

Printer-friendly Version

Interactive Discussion

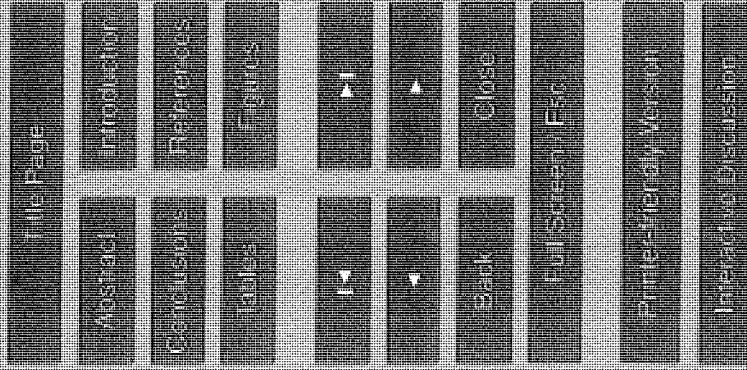


to approximately 262 m composite depth were used for clustering in 4 different groups (Clusters I to IV) ^{statistical} (using ^{method} again k-mean clustering). For interpretation of the statistically derived clusters, the described facies type was assigned to all samples. Given that sampling occurred generally in 2-cm-steps (Melles et al., 2012), we used the facies type at the mean depth of the sample as representative for the entire sample, neglecting that facies boundaries could also occur within a discrete sample.

4 Seismic and petrophysical description of the entire lithological succession

4.1 Seismic profiles

For the description of the seismic sections, we follow the stratigraphic numbering introduced by Gebhardt et al. (2006). This numbering is based on a depth-velocity model derived from seismic refraction data. We use Unit I for lacustrine sediments, and Unit II and III for the underlying suevite layer and the brecciated bedrock that form the basement of the lake ^{below the lake floor} and that were deformed by the impact. Seismic reflection data exhibit that Unit I can be subdivided into an upper, well-stratified Subunit Ia and a lower, more chaotic sedimentary Subunit Ib (Fig. 2). Acoustic velocities are around 1550 to 1650 ms⁻¹ for both Subunits, ^{indicating} pointing at unconsolidated sediments. This is confirmed by the sedimentary record of ICDP site 5011-1 (Melles et al., 2011). Subunit Ia has a relatively flat surface in large parts of the basin, but the bathymetry is sometimes rough in the more proximal areas where mass movement deposits occur frequently in the upper layers or on top of the sediments. Mass movement deposits are quite common mainly in the proximal parts of the lake in both Subunits Ia and Ib (e.g. Juschus et al., 2009; Niessen et al., 2007; Sauerbrey et al., 2013), and even in the lake center at the distal 5011-1 drill site, ^{where} they make up approximately one third of the entire sediment column (Sauerbrey et al., 2013). In the lower part of Subunit Ia, mass movement deposits reach much further ^{further} towards the central part of the lake (Fig. 2), whereas in the upper layers, they are almost entirely restricted to the proximal part of the lake. This is



confirmed by the fact that only small mass movement deposits, mainly turbidites, were found in pilot cores PG1351 (~13 m length) (Melles et al., 2007) and LZ1024 (~16 m length) (Juschnus et al., 2009). The turbidites were associated with distant debris flows in a conceptual model by Juschnus et al., 2009, and their interdependence is confirmed by findings in the drill cores by Sauerbrey et al. (2013). *please clarify*

The wide shelf at the southeastern part of the lake is characterized by aggrading sequences; seismic data from the western and northwestern shelf are not available due to coarse sediments limiting acoustic penetration in these areas. Subunit Ia forms onlaps against the steep slope at the lake margins in a layer-cake manner (Fig. 2), gradually muting a formerly deeper and steeper relief (Niessen et al., 2007). Subunit Ia conformably overlies Subunit Ib with a clear and distinct boundary ^{the two} between Subunit Ib has a massive, acoustically chaotic character and rarely shows internal layering in ~~these parts~~ that are visible in ^{the} seismic profiles. Its upper boundary has a hummocky surface probably due to thick, chaotic mass movements in its uppermost parts (Fig. 2). Its lower boundary to Unit II lies below the acoustic multiples and is therefore masked. However, refraction data showed that Subunit Ib drapes the central uplift structure ~~that was observed in the seismic refraction data in Units II and III~~ and that is characteristic for impact craters of this size (Gebhardt et al., 2006).

Faults with a vertical offset of up to several meters were observed in the central part of the northern profiles in Unit I. These show a decreasing offset towards the more recent sediment and are inactive in the upper meters of the lake sediments (Fig. 2); this was also observed in high-resolution subbottom profiles (Niessen et al., 2007). The faults are likely related to the central uplift structure *later settling and subsidence of*.

4.2 Physical properties from downhole and core measurements

Subunit Ia comprises the uppermost ~167 m of the sediment column (Fig. 3), which corresponds to approximately 3.17 Ma (Nowaczyk et al., 2013). This also includes the Pliocene/Pleistocene transition at 123 m b.l.f. (2.6 Ma). Downhole logging data show that the Pleistocene sediments are characterized by relatively constant K and Th

This Page

Abstract

Introduction

Conclusions

References

Tables

Figures

◀

▶

◀

▶

Back

Close

Full Screen/ Esc

Printer Friendly Version

Interactive Discussion



counts down to approximately 100 m b.l.f. (2.1 Ma, Nowaczyk et al., 2013); magnetic susceptibilities of the sediment core are highly variable, but fluctuate in a range between ~ 15 and $\sim 200 \times 10^{-4}$ SI (Fig. 3). Similarly to magnetic susceptibility, density is highly variable throughout the entire record, but scatters ~~constantly~~ around a mean value of approximately 1.5 g cm^{-3} in the sediments of Subunit 1a (< 3.17 Ma). Lithologies and associated sedimentary facies are characterized by a rapid change between homogeneous (Facies B) and laminated (Facies A) layers that represent warm and cold phases, respectively (Melles et al., 2007), as well as occasional laminated sediments reflecting peak warm conditions (Facies C). These hemipelagic sediments are intercalated by a large number of mass movement deposits of different types such as debris flows and turbidites (Sauerbrey et al., 2013) that ~~get thicker towards the~~ lower boundary of Subunit 1a (Fig. 3). Below 100 m b.l.f., downhole logging K and Th counts show an increase with increasing depth with the highest values exactly at the Pliocene/Pleistocene boundary and strongly decreasing values in the uppermost part of the Pliocene sediments. Magnetic susceptibility values of the Pliocene part of Subunit 1a show a slight increase in amplitude in comparison to the Pleistocene data.

Subunit 1b comprises all lacustrine sediments between 167 m b.l.f. and the boundary to the underlying bedrock at ~ 320 m b.l.f. While magnetic susceptibility values of the Pleistocene part of Subunit 1a originate from sediment core measurements (MS, light blue in Fig. 3), the values of the Pliocene ~~part~~ ^{section} were measured in the borehole (BMS, dark blue). The two datasets are not completely comparable in terms of their exact values and amplitudes; at first glance, it seems as if the lower part has much higher amplitudes, this however might be an artefact caused by the different measurement methods. Magnetic susceptibility seems to be more variable in longterm trends in the Pliocene part of the sediments; however, it is unclear if this is a real paleoclimate signal or just a scaling effect. Unfortunately, there is not enough overlap in between the two datasets to tune them to similar amplitudes. Nevertheless, it is obvious that magnetic susceptibility is much more variable between approximately 150 and 220 m b.l.f. than below (220 m corresponds to 3.38 Ma, Nowaczyk et al., 2013). Electrical resistivity is

rather constant throughout the entire Pliocene sediment succession with exception of the lowermost approximately 20 m where a small maximum occurs at ~300 m b.l.f. Density shows an increase with increasing depth from mean values around 1.5 g cm^{-3} in the uppermost part of Subunit Ib to mean values around 1.8 g cm^{-3} with values as high as $> 2.0 \text{ g cm}^{-3}$ in the lowermost part, i.e. in the transitional zone between lacustrine and impact-related units. Lithological description of Subunit Ib is not as detailed as for Subunit Ia due to lower recovery and, thus, larger drilling-related gaps (for details on drillings operations, see Melles et al., 2011). As in the upper part, sediments are alternating between Facies A and B, but the homogeneous facies B is much more dominating in the Pliocene part of the record. Only in the lowermost part, i.e. below ~270 m b.l.f. (3.48 Ma, Nowaczyk et al., 2013), laminated sediments are more abundant. As in Subunit Ia, mass movement deposits are intercalated frequently in the hemipelagic sediments.

Uranium values are rather constant throughout the entire record with slightly higher values in the bedrock. Two strong exceptions however are observed in the lacustrine part: (a) between ~220 and ~244 m b.l.f., U values are slightly enhanced, and (b) a strong double peak is observed between ~251 and ~262 m b.l.f. The U peaks are confirmed by the independently measured total GR.

Electrical resistivity (deep and shallow), borehole magnetic susceptibility, and natural gamma ray counts of K, U and Th were used for cluster analyses to distinguish between different main units between 143 m and 394 m b.l.f. This includes the boundary between the lacustrine sediments and the brecciated bedrock. Three clusters could be distinguished: (1) Cluster 1 is characterized by high electrical resistivity and enhanced K content values (Fig. 4 upper panel). Magnetic susceptibility is rather variable. (2) Cluster 2 is characterized by low electrical resistivity, variable magnetic susceptibility, and low U and K content. (3) Cluster 3 has low electrical resistivity, high U and intermediate K values (Fig. 4 upper panel). It is clearly different from Cluster 2 in almost all parameters, but coincides with Cluster 2 in terms of low resistivity. Plotting these three clusters against depth (Figs. 3 and 5), it becomes obvious that Cluster 1 clearly describes

the bedrock. Cluster 2 comprises the main part of the lacustrine record. Cluster 3 is part of the lacustrine sediments, but only comprises the section between 254.44 and 259.15 m b.l.f. and between 260.7 and 262.5 m b.l.f. where the strong U double-peak is observed (Fig. 3).

Both pelagic sediments and mass movement deposits in Lake El'gygytyn are part of clusters 2 and 3, which implies that these two sediment types do not differ in their petrophysical characteristics. This confirms that the mass movement deposits ~~mainly~~ consist of reworked lacustrine material (Sauerbrey et al., 2013). Enhanced U values in cluster 3 found in the borehole data could not be measured with the ITRAX XRF core scanner in the according core sections, probably due to the scanner's ~~low capa-~~^{limited ability} bility in measuring U. U is removed from the water column and buried in the sediment during oxic conditions (e.g. Anderson et al., 1989); this would probably point at high bottom water oxygen levels when these layers ^{which} were accumulated. This, however, is not confirmed by the sediment description, ~~that~~ ^{which} does not differ significantly from above or below these layers. Hence, it is more likely that U-rich rocks were eroded in the lake catchment during these periods and transported to the lake by fluvial/eolian rather than gravitational transport processes.

Natural gamma radiation is often measured and used as an indicator for clay content in sediments, using the fact that K and Th are enriched in different clay minerals. This approach, however, does not work in Lake El'gygytyn sediments where clay K and Th do not correlate with clay or any other grain size (2013) neither with the spectral gamma nor with the total gamma dataset (Eqs. 1–4, respectively). This can best be explained by the lake's location in a small catchment with short transport paths from the source rock to the accumulation site, which prohibits full weathering of all grains. K-bearing feldspar grains that would normally weather into K-bearing clay, so K would be an indicator for clay solely. In the case of a very short distance from source to sink, K-bearing feldspar grains of probably fine sand or silt size would also end up in the sediment along with clay. This would in turn ~~mean~~^{show} that the assumption that sand does not contain K (see Eq. 1, methods chapter) is wrong in our case.

Petrophysical characterization of the lacustrine sediment succession

A. C. Gebhardt et al.

The Page

Abstract

Introduction

Conclusions

References

Tables

Figures

1

2

3

4

Back

Close

Full Screen / Esc

Printer-friendly Version

Interactive Discussion



4.3 Physical properties from downhole and core measurements

The most prominent change in the downhole logging data occurs at the boundary between lacustrine sediments and the underlying altered bedrock at ~ 320 m b.l.f. (Figs. 3, 5). While sediments above ~ 313 m b.l.f. are clearly lacustrine with alternating homogeneous and laminated layers, intercalated with frequent mass movement deposits, sediments below ~ 313 m b.l.f. are a mixture between a sedimentary matrix and reworked impact breccia. The boundary ~~is~~ between the lacustrine sediments and the underlying bedrock is thus rather a transitional zone than a sharp boundary. In the upper part of this transitional zone, i.e. ~ 313 and 319.8 m b.l.f. (transitional zone T1 in Fig. 5), lacustrine sediments form the dominant part of the record, while below 319.8 m b.l.f. (T2 and T3) the record contains mainly reworked impact breccia in a sedimentary matrix (Raschke et al., 2012). Therefore, the formal boundary between the lacustrine and the impact part of the drill core was defined at 319.8 m b.l.f., between drill runs 97Q and 98Q. Koeberl et al. (2012) subdivide the part of the transitional zone that lies below this boundary into two subunits, one from 319.8 to 323 (T2 in Fig. 5) and the second from 323 to 331 m b.l.f. (T3) (note that the original depth values from both Raschke et al. (2012) and Koeberl et al. (2012) were shifted downwards by 3 m to match the depth scale used by the lacustrine El'gygytyn scientific community). Both subunits show similar lithologies with fine sand-sized grains mainly composed of glass fragments, intercalated with impact breccia and impact melt blocks. All three subunits of the transitional zone (T1 above, T2 and T3 below the formal boundary) are shown in light to dark grey tones of facies type E in Fig. 5. The boundary between the matrix-dominated (= lacustrine, T1) and the clast-dominated (= impact-related, T2 and T3) part shows ~~up~~ as a sharp boundary in the electrical resistivity and also in the magnetic susceptibility data. Nevertheless, cluster analyses shows that except for two small bands, the entire transitional zone exhibits characteristics that are more similar to the overlying lacustrine succession. Only below this transitional zone, the sediments are clearly of bedrock-type ^{affinity}.

Title Page

Abstract

Introduction

Conclusions

References

Tables

Figures

1

▶

◀

▶

Back

Close

Full Screen / Esc

Printer-friendly Version

Interactive Discussion



Chemical elements K and Th are enriched just above our formal bedrock-lake sediment boundary, but depleted below with exception of the lowermost part of the transitional zone. Below 331 m b.l.f., a long succession of suevite was described by Raschke et al. (2012) and by Koeberl et al. (2012). The suevite is obviously petrophysically not homogeneous with highly variable values in both electrical resistivity and magnetic susceptibility (Fig. 5). Two volcanic-like blocks (336.83 to 340 and 354 to 353 m b.l.f.), as well as an ignimbrite block (386 to 388.5 m b.l.f.) described by Koeberl et al. (2012) correspond to peaks in the electrical resistivity data (Fig. 5). Electrical resistivity shows a decreasing trend inside the upper volcanic block towards lower depths, while the opposite is observed in the ignimbrite layer. The former plots into the lacustrine cluster not because it is of lacustrine origin, but quite likely because it differs from the surrounding bedrock; the latter seems to be similar to the surrounding bedrock. Furthermore, electrical resistivity shows that the thick suevite layers have some pronounced internal layers of apparently different geophysical character.

5 Variability in the lacustrine succession

5.1 Description of the lacustrine succession

While electrical resistivity shows pronounced peaks in the bedrock and in the transitional zone, it is ~~pretty~~ ^{fairly} constant with only very small peaks throughout the entire lacustrine section, exhibiting some smaller but smooth shifts ^{only} in the lowermost part only (Figs. 3 and 5). This ~~points~~ ^{points} at a rather uniform succession of sediments without abrupt changes, even though the sediments are highly variable and change rapidly between homogeneous and laminated layers and mass movement deposits (see facies column in Fig. 3). This is reflected in the fact that almost the entire lacustrine succession is represented by cluster 2 with only a very small ^{part} ~~portion~~ that has extraordinary high U values clustering separately into cluster 3 (Fig. 3). The apparent discrepancy between a highly variable sediment and still quite similar petrophysical characteristics can also be best

explained by the lake's location in a rather small catchment of only 293 km² (including the lake's surface) (Nolan and Brigham-Grette, 2007). This ^{50-55%} means that during warmer as well as during colder periods the same source rock is eroded, and thus all clastic grains that end up in the lacustrine sediments (probably with exception of some eolian grains; these however are a minor contribution to the sediment, see Francke et al., 2013; Fedorov et al., 2013) originate from the same provenance. Nevertheless, differing erosional processes (i.e. more physically-dominated weathering during colder and more chemically-dominated weathering during warmer periods) in the small hinterland as well as diatom blooms during warmer periods are strong enough to generate highly variable sediment properties (cf. Minyuk et al., 2007) ^{identical} with yet almost similar character in terms of petrophysical characteristics. Magnetic susceptibility, in turn, is highly variable in the lacustrine part, probably reflecting different weathering mechanisms and ~~definitely~~ different modes of palaeohydrological conditions (such as anoxia in the bottom water, see Melles et al., 2007, 2012) along with dilution effects by biogenic material.

In order to detect the variability within the lacustrine succession related to the different modes in paleoenvironmental conditions, we carried out clustering analyses on 5538 data points using similar parameters as in Melles et al. (2007, 2012). With Si/Ti ratio, TOC percentage and magnetic susceptibility from core measurements, we were able to identify four clusters (Tables 1 and 2): "Cluster I" is defined by medium TOC percentages, very low Si/Ti ratios and very low magnetic susceptibility. "Cluster II" shows high TOC percentages along with high Si/Ti ratios and medium magnetic susceptibility. "Cluster III" has low TOC percentages and medium Si/Ti ratios along with high magnetic susceptibility. "Cluster IV" is defined by low TOC percentages and Si/Ti ratios combined with high magnetic susceptibility. Density does not vary ^{significantly} much between Clusters I, III and IV, but is considerably lower in Cluster II.

Revised 251-391, 2013

Remains separate for each

Petrophysical characterization of the lacustrine sediment succession

A. C. Gebhardt et al.

Table of Contents

Abstract

Introduction

Conclusions

References

Figures

Back

Close

Full Screen Esc

Printer-friendly Version

Interactive Discussion



5.2 Description of the lacustrine succession

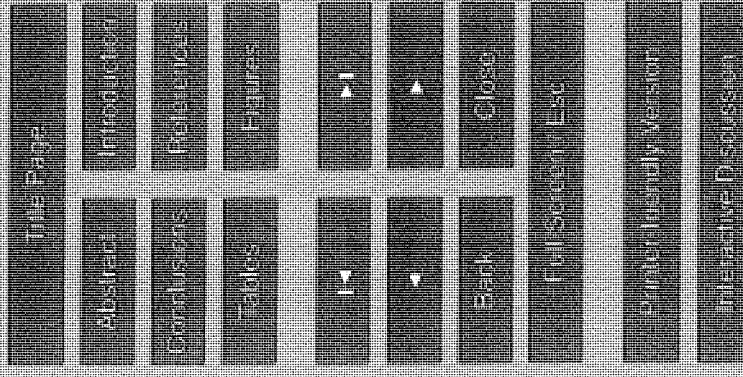
Melles et al. (2007, 2012) used TOC percentage, Si/Ti content and magnetic susceptibility to identify the oxygenation state of the bottom water and, thus, whether the water column was mixed or stratified, which in turn gives evidence on the duration of an ice cover on the lake. During phases with a perennial ice cover, the water column could not mix, and depletion of oxygen in the bottom water lead to enhanced preservation of organic material, while magnetite underwent dissolution, leading to reduced magnetic susceptibility values. ^{Ti content?} During times with seasonal ice cover, ~~in contrast~~, mixing of the water column was possible during summer months (as it is today, see Nolan and Brigham-Grette, 2007). Organic carbon was thus consumed in the oxic bottom water, and magnetic minerals were buried without alteration (Melles et al., 2007, 2012). Si/Ti ratios can be used to estimate the biogenic vs. clastic input to the lake (Melles et al., 2012; Wennrich et al., 2013). Enhanced Si/Ti values ^{50-100%} point at high biogenic silica contents, which in the case of Lake El'gygytyn are produced by enhanced primary productivity, ~~here~~ ^{indicate} mainly diatoms, during warmer times with only seasonal ice cover. Low Si/Ti values point at colder periods with perennial ice cover, thus limitation in light penetration necessary for photosynthesis, along with probably enhanced clastic input through the 50 small ephemeral inlets around the lake (Melles et al., 2007, 2012). During times with a perennial ice cover, clastic input is triggered by seasonal moats and vertical conduits in the ice. ^{As} is the case today when snow melt starts in late spring, see Nolan et al., 2003; Asikainen et al., 2007; Francke et al., 2013).

Using this information, we can plot the clusters in a redox-condition vs. input-type diagram (Fig. 6). In such a diagram, the different modes of paleoenvironmental conditions known from earlier studies by Melles et al. (2007, 2012) can be visualized as shown in Figs. 6e, f: the glacial modes of Facies A with perennial ice cover and a stratified water column would plot into the upper left corner (anoxic conditions, dominated by clastic input or by a relative dominance of clastic material due to the lack of biogenic input); the interglacial mode of Facies B with seasonal ice cover and a mixed water column

9, 351–391, 2013

Petrophysical characterization of the lacustrine sediment succession

A. C. Gebhardt et al.



plots

would show-up in the right middle part (oxic conditions with variable, but intermediate contents of clastic and biogenic input), and Facies C – the super interglacial mode – would be found in the lower middle with with variably suboxic and oxic conditions and a dominance in biogenic input.

5 When plotting Clusters I to IV into this diagram (Fig. 6), it becomes obvious that sediments of Facies B, i.e. the interglacial sediments, plot into several clusters (Fig. 6a to d): a high portion of Facies B sediments are found in Cluster IV (62.25 % of all Facies B data points), and another 29.59 % plot in Cluster III. In Cluster I and II, some minor (5.27 % and 2.90 %) of Facies B sediments are found. This supports the earlier study by Melles et al. (2012) that describes Facies B sediments as highly variable.

10 Facies F, i.e. the mass movement deposits, also plot into all clusters with the majority in Cluster IV (80.39 %). Almost equal percentages of 10.98 % and 8.24 % plot into Clusters III and II, and negligible 0.39 % is found in Cluster I. As Facies F is not part of the hemipelagic sediments in Lake El'gytgytn, it was omitted in the pie plots in Fig. 6 for better visualization of the distribution of Facies types A to D in the different clusters. The fact that both Facies F and Facies B only have minor parts plotting into Clusters I and II, along with the fact that these clusters only represent 13.01 % and 4.51 % of all data points, suggests that these two clusters might represent sediment endmembers of Lake El'gytgytn.

15 "Glacial" Cluster I (687 data points = 13.01 % of entire dataset, Fig. 6a) plots into a field where sediments of Facies A and some of Facies B would be assumed. It contains equal amounts (30.86 % and 30.13 %) of both "cold & dry" Facies A_d and "cold & moist" Facies A_m. Another 30.42 % of this cluster comprises sediments that were classified as Facies B, i.e. sediments interpreted as accumulated during interglacials, and some 5.82 % were even described as from super interglacials (Facies C). This means that sediments of Facies A show similar characteristics as a certain portion of Facies B sediments, so they could not be statistically separated by means of cluster analysis. Nevertheless, the portion of Facies B data that plot into Cluster I is only 5.27 % of all Facies B data (Fig. 6a) and might even be negligible. In fact, samples used

Petrophysical characterization of the lacustrine sediment succession

A. C. Gebhardt et al.

Title Page

Abstract

Introduction

Conclusions

References

Tables

Figures

◀

▶

◀

▶

Back

Close

Full Screen / Esc

Printer-friendly Version

Interactive Discussion



for this study are generally 2 cm thick, and we chose the facies type of their average composite depth as representative for the entire 2 cm, neglecting that facies boundaries might occur also within samples. Plotting facies types and clusters versus depth (Fig. 7) reveals that Cluster I quite well captures the cold phases, marked with light and dark blue bars for example at ~ 52.5 to 52.9 m b.l.f., at ~ 53.4 to 53.5 m b.l.f. and at 63.9 to 64.5 m b.l.f.

“Interglacial” Clusters III and IV: Cluster III (1444 data points = 27.34 % of entire dataset, Fig. 6c) as well as Cluster IV (2912 data points = 55.15 % of the entire dataset, Fig. 6b) have very low TOC contents and high magnetic susceptibility values, pointing at oxic bottom water conditions during their deposition. While in Cluster IV Si/Ti ratios are low, slightly higher Si/Ti ratios in Cluster III suggest some biogenic input into the sediment. A high portion of Cluster IV is composed of Facies B sediment (84.82 %), and equal parts of 6.25 and 6.11 % consist of Facies A_d and C, respectively. In Cluster IV, which is the largest cluster and contains more than half of all data points, also Facies B is clearly dominant with 81.30 %, and 12.74 % are made up of Facies C type sediments along with some 4.02 % of Facies A_d. Both clusters contain the majority of all Facies B data points and confirm that this facies type is rather variable yet similar, being deposited under oxic conditions. The Facies A_d sediments found in these two clusters, however, suggest that even during glacial times, oxic (or at least suboxic) conditions in the bottom water were sometimes encountered at least during periods with “cold & dry” conditions, and some bioproduction leading to enhanced Si/Ti ratios was possible. This is in good agreement with findings by Melles et al. (2007; 2012) who suggested that “cold & dry” Facies A_d represents a perennial ice cover without snow cover. This would allow some light penetration and thus some primary productivity in the water column. In contrast, “cold & moist” Facies A_m was interpreted as representing a perennial ice cover covered by snow, inhibiting any light penetration into the water column, leading to only very limited photosynthetic life in the lake and thus low TOC values and Si/Ti ratios. This, in turn, is confirmed by only negligible 0.58 and 0.07 % of Facies A_m in Clusters III and IV, and 0.84 % in Cluster II.

Petrophysical characterization of the lacustrine sediment succession

A. C. Gebhardt et al.

This Page

Abstract

Introduction

Conclusions

References

Tables

Figures

1

2

3

4

Back

Close

Full Screen / Esc

Printer-friendly Version

Interactive Discussion



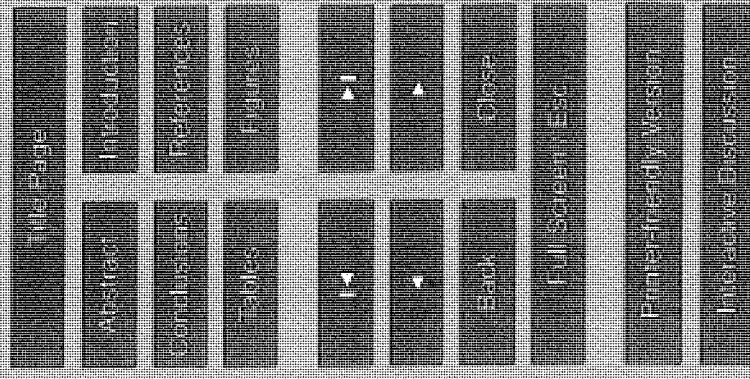
“Super interglacial” Cluster II (238 data points = 4.51 % of the entire dataset; Fig. 6g): cluster II has significantly enhanced TOC and Si/Ti ratios and consists to almost equal parts of Facies C and B sediments (47.48 % and 48.32 %). The negligible remainder is 3.36 % Facies D and 0.84 % Facies A_m.

While density is rather variable in Clusters I, III and IV, it is clearly lower than average in Cluster II, which is in good agreement with a high content of biogenic silica. Even though approximately half of Cluster II consists of Facies C type sediments, only approximately one fifth of all Facies type sediments plot into this cluster (21.94 %), while some 35.73 and 43.56 % plot into Clusters III and IV. This might either point at a wider range of TOC percentages, Si/Ti ratio and magnetic susceptibility values within this facies type, or these samples are highly biased by facies changes within the distinct samples that led to a wrong assignment of facies type to a specific sample. When plotting facies and clusters together vs. depth (Fig. 7) it becomes obvious that only some parts of Facies C (red bars) were captured by Cluster II: between ~62 and ~62.7 m b.l.f., Facies C sediments were visually described, but have rather low Si/Ti content and only slightly enhanced TOC values, so they were statistically gathered into Clusters I and IV; these samples are part of the 5.82 % of Facies C samples that were found in Cluster I and 6.11 % in Cluster IV. On the other hand, sediments of the thick Facies C layer between ~64.7 and ~65.6 m b.l.f. show higher Si/Ti ratios and TOC content and were therefore gathered into Clusters III and II. This would imply that even though Facies C is easily detected by means of visual core description, its basic physical and geochemical properties might not always be significantly different from sediments of other facies types, notably from Facies B. Nevertheless, this is in good agreement with findings by Melles et al. (2012) who report that while primary productivity was highest during these extraordinary phases, there are laminae found in the Facies C sediments that suggest at least seasonally suboxic or anoxic conditions in the bottom waters. This could result in a wide variety of TOC percentages and magnetic susceptibility values in the according sediment and make it difficult to gather these sediments in one single cluster.

Resulting

Petrophysical characterization of the lacustrine sediment succession

A. C. Gebhardt et al.



6 Conclusions

Seismic reflection profiles of Lake El'gygytyn exhibit mostly well-stratified sediments with frequent mass movement deposits intercalated in the more proximal areas. The well-stratified acoustic layers are ~~highly~~ ^{correlated with} confirmed by the well-layered sediments of the drill core retrieved during winter/spring 2009, with highly variable facies types changing at high frequency in the core. The lacustrine sediment succession can be separated into two seismic subunits Ia and Ib. ^{whereas} Ia is well-stratified, Ib is acoustically more chaotic. The sediment-bedrock boundary was identified earlier by Gebhardt et al. (2006) at around 320 to 330 m b.l.f. by means of a seismic-refraction data derived depth-velocity model. This was confirmed during drilling with the first bedrock material found at approximately 320 m b.l.f. Downhole logging data down to 394 m b.l.f., i.e. through the entire lacustrine column and some 74 m into the bedrock, show that the lacustrine and bedrock part ^{and distinction is} (differ clearly) in their petrophysical characteristics: Cluster analysis separates three clusters, two of which comprise the entire lacustrine succession, while the third contains the bedrock. The boundary between the impact-related bedrock and the lacustrine succession is not sharp, but rather a transitional zone with an upwards increasing portion of lacustrine material. Potassium and resistivity values are enhanced in the bedrock ~~part~~ ^{section}.

In the lacustrine succession, a prominent U peak of unknown origin is visible at around 255 m b.l.f., and slightly enhanced Th and K values mark the Pliocene/Pleistocene transition. The core could be clustered into four different clusters (I to IV) down to approximately 262 m composite depth. The clusters show significant differences in terms of their TOC percentage, Si/Ti ratio and magnetic susceptibility, in some cases also density. This allows plotting the clusters into a redox-condition vs. input-type diagram. In comparison with earlier studies we ~~could~~ conclude that Cluster I contains glacial sediments, III and IV sediments from interglacials, and II comprises the sediments from super interglacial ^{intervals}.

9, 351–391, 2013

Petrophysical characterization of the lacustrine sediment succession

A. C. Gebhardt et al.

This Page

Abstract

Introduction

Conclusions

References

Tables

Figures

1

2

3

4

Back

Close

Full Screen / Esc

Printer-friendly Version

Interactive Discussion



Discussion Paper

Discussion Paper

Discussion Paper

Discussion Paper